

# Probability distribution of returns in the Heston model with stochastic volatility\*

Adrian A Drăgulescu<sup>1</sup> and Victor M Yakovenko<sup>2</sup>

Department of Physics, University of Maryland, College Park,  
MD 20742-4111, USA

E-mail: adrian.dragulescu@constellation.com and  
yakovenk@physics.umd.edu

Received 11 March 2002, in final form 22 October 2002

Published 2 December 2002

Online at [stacks.iop.org/Quant/2/443](http://stacks.iop.org/Quant/2/443)

## Abstract

We study the Heston model, where the stock price dynamics is governed by a geometrical (multiplicative) Brownian motion with stochastic variance. We solve the corresponding Fokker–Planck equation exactly and, after integrating out the variance, find an analytic formula for the time-dependent probability distribution of stock price changes (returns). The formula is in excellent agreement with the Dow–Jones index for time lags from 1 to 250 trading days. For large returns, the distribution is exponential in log-returns with a time-dependent exponent, whereas for small returns it is Gaussian. For time lags longer than the relaxation time of variance, the probability distribution can be expressed in a scaling form using a Bessel function. The Dow–Jones data for 1982–2001 follow the scaling function for seven orders of magnitude.

## 1. Introduction

Stochastic dynamics of stock prices is commonly described by a geometric (multiplicative) Brownian motion, which gives a log-normal probability distribution function (PDF) for stock price changes (returns) [1]. However, numerous observations show that the tails of the PDF decay slower than the log-normal distribution predicts (the so-called ‘fat-tails’ effect) [2–4]. Particularly, much attention was devoted to the power-law tails [5, 6]. The geometric Brownian motion model has two parameters: the drift  $\mu$ , which characterizes the average growth rate, and the volatility  $\sigma$ , which characterizes the noisiness of the process. There is empirical evidence and a set of stylized facts indicating that volatility, instead of being a constant parameter, is driven by a mean-reverting stochastic

process [7, 8]. Various mathematical models with stochastic volatility have been discussed in the literature [9–15].

In this paper, we study a particular stochastic volatility model, called the Heston model [11], where the square of the stock price volatility, called the variance  $v$ , follows a random process known in financial literature as the Cox–Ingersoll–Ross (CIR) process and in mathematical statistics as the Feller process [8, 16]. Using the Fourier and Laplace transforms [14, 16], we solve the Fokker–Planck equation for this model exactly and find the joint PDF of returns and variance as a function of time, conditional on the initial value of variance. While returns are readily known from financial time series data, variance is not given directly, so it acts as a hidden stochastic variable. Thus, we integrate the joint PDF over variance and obtain the marginal PDF of returns *unconditional* on variance. The latter PDF can be directly compared with financial data. We find an excellent agreement between our results and the Dow–Jones data for the 20 year period of 1982–2001. Using only four fitting parameters, our equations very

\* Paper presented at Applications of Physics in Financial Analysis (APFA) 3, 5–7 December 2001, Museum of London, UK.

<sup>1</sup> Present address: Constellation Energy Group, Baltimore, MD, USA.

<sup>2</sup> <http://www2.physics.umd.edu/~yakovenk>

well reproduce the PDF of returns for time lags between 1 and 250 trading days. In contrast, in ARCH, GARCH, EGARCH, TARCH, and similar models, the number of fitting parameters can easily go to a few tens [17].

Our result for the PDF of returns has the form of a one-dimensional Fourier integral, which is easily calculated numerically or, in certain asymptotical limits, analytically. For large returns, we find that the PDF is exponential in log-returns, which implies a power-law distribution for returns, and we calculate the time dependence of the corresponding exponents. In the limit of long times, the PDF exhibits scaling, i.e. it becomes a function of a single combination of return and time, with the scaling function expressed in terms of a Bessel function. The Dow–Jones data follow the predicted scaling function for seven orders of magnitude.

The original paper [11] solved the problem of option pricing for the Heston model. Numerous subsequent studies [13–15, 18] compared option pricing derived from this model and its extensions with the empirical data on option pricing. They found that the Heston model describes the empirical option prices much better than the Black–Scholes theory, and modifications of the Heston model, such as adding discontinuous jumps, further improve the agreement. However, these papers did not address the fundamental question whether the stock market actually follows the Heston stochastic process or not. Obviously, if the answer is negative, then using the Heston model for option pricing would not make much sense. The stock market time series was studied in [15] jointly with option prices, but the focus was just on extracting the effective parameters of the Heston model. In contrast, we present a comprehensive comparison of the stock market returns distribution with the predictions of the Heston model. Using a single set of four parameters, we fit the whole family of PDF curves for a wide variety of time lags. In order to keep the model as simple as possible with the minimal number of fitting parameters, we use the original Heston model and do not include later modifications proposed in the literature, such as jumps, multiple relaxation time, etc [13–15]. Interestingly, the parameters of the model that we find from our fits of the stock market data are of the same order of magnitude as the parameters extracted from the fits of option prices in [13–15].

## 2. The model

We consider a stock, whose price  $S_t$ , as a function of time  $t$ , obeys the stochastic differential equation of a geometric (multiplicative) Brownian motion in the Itô form [1, 19]:

$$dS_t = \mu S_t dt + \sigma_t S_t dW_t^{(1)}. \quad (1)$$

Here the subscript  $t$  indicates time dependence,  $\mu$  is the drift parameter,  $W_t^{(1)}$  is a standard random Wiener process<sup>3</sup>, and  $\sigma_t$  is the time-dependent volatility.

Since any solution of (1) depends only on  $\sigma_t^2$ , it is convenient to introduce the new variable  $v_t = \sigma_t^2$ , which is

<sup>3</sup> The infinitesimal increments of the Wiener process  $dW_t$  are normally distributed (Gaussian) random variables with zero mean and the variance equal to  $dt$ .

called the variance. We assume that  $v_t$  obeys the following mean-reverting stochastic differential equation:

$$dv_t = -\gamma(v_t - \theta) dt + \kappa \sqrt{v_t} dW_t^{(2)}. \quad (2)$$

Here  $\theta$  is the long-time mean of  $v$ ,  $\gamma$  is the rate of relaxation to this mean,  $W_t^{(2)}$  is a standard Wiener process, and  $\kappa$  is a parameter that we call the variance noise. Equation (2) is known in financial literature as the CIR process and in mathematical statistics as the Feller process [8, 16]. Alternative equations for  $v_t$ , with the last term in (2) replaced by  $\kappa dW_t^{(2)}$  or  $\kappa v_t dW_t^{(2)}$ , have also been discussed in the literature [9]. However, in our paper, we study only the case given by equation (2).

We take the Wiener process appearing in (2) to be correlated with the Wiener process in (1):

$$dW_t^{(2)} = \rho dW_t^{(1)} + \sqrt{1 - \rho^2} dZ_t, \quad (3)$$

where  $Z_t$  is a Wiener process independent of  $W_t^{(1)}$ , and  $\rho \in [-1, 1]$  is the correlation coefficient. A negative correlation ( $\rho < 0$ ) between  $W_t^{(1)}$  and  $W_t^{(2)}$  is known as the leverage effect [8, p 41].

It is convenient to change the variable in (1) from price  $S_t$  to log-return  $r_t = \ln(S_t/S_0)$ . Using Itô's formula [19], we obtain the equation satisfied by  $r_t$ :

$$dr_t = \left( \mu - \frac{v_t}{2} \right) dt + \sqrt{v_t} dW_t^{(1)}. \quad (4)$$

The parameter  $\mu$  can be eliminated from (4) by changing the variable to  $x_t = r_t - \mu t$ , which measures log-returns relative to the growth rate  $\mu$ :

$$dx_t = -\frac{v_t}{2} dt + \sqrt{v_t} dW_t^{(1)}. \quad (5)$$

Where it does not cause confusion with  $r_t$ , we use the term ‘log-return’ also for the variable  $x_t$ .

Equations (2) and (5) define a two-dimensional stochastic process for the variables  $x_t$  and  $v_t$  [11, 14]. This process is characterized by the transition probability  $P_t(x, v|v_i)$  having log-return  $x$  and variance  $v$  at time  $t$  given the initial log-return  $x = 0$  and variance  $v_i$  at  $t = 0$ . Time evolution of  $P_t(x, v|v_i)$  is governed by the Fokker–Planck (or forward Kolmogorov) equation [19]

$$\begin{aligned} \frac{\partial}{\partial t} P = \gamma \frac{\partial}{\partial v} [(v - \theta) P] + \frac{1}{2} \frac{\partial}{\partial x} (v P) \\ + \rho \kappa \frac{\partial^2}{\partial x \partial v} (v P) + \frac{1}{2} \frac{\partial^2}{\partial x^2} (v P) + \frac{\kappa^2}{2} \frac{\partial^2}{\partial v^2} (v P). \end{aligned} \quad (6)$$

The initial condition for (6) is a product of two delta functions

$$P_{t=0}(x, v|v_i) = \delta(x)\delta(v - v_i). \quad (7)$$

The probability distribution of the variance itself,  $\Pi_t(v) = \int dx P_t(x, v)$ , satisfies the equation

$$\frac{\partial}{\partial t} \Pi_t(v) = \frac{\partial}{\partial v} [\gamma(v - \theta) \Pi_t(v)] + \frac{\kappa^2}{2} \frac{\partial^2}{\partial v^2} [v \Pi_t(v)], \quad (8)$$

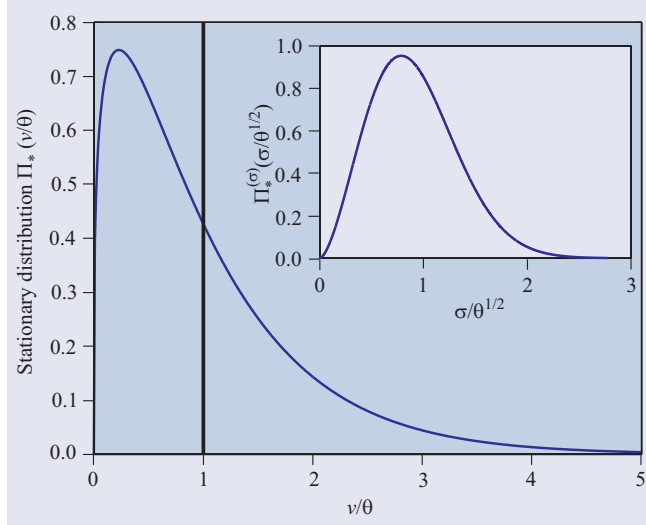


**Figure 1.** The stationary probability distribution  $\Pi_*(v)$  of variance  $v$ , given by equation (9) and shown for  $\alpha = 1.3$  from table 1. The vertical line indicates the average value of  $v$ . Inset: the corresponding stationary probability distribution  $\Pi_*^{(\sigma)}(\sigma)$  of volatility  $\sigma$  given by equation (10).

which is obtained from (6) by integration over  $x$ . Feller [16] has shown that this equation is well-defined on the interval  $v \in [0, +\infty)$  as long as  $\theta > 0$ . Equation (8) has the stationary solution

$$\Pi_*(v) = \frac{\alpha^\alpha}{\Gamma(\alpha)} \frac{v^{\alpha-1}}{\theta^\alpha} e^{-\alpha v/\theta}, \quad \alpha = \frac{2\gamma\theta}{\kappa^2}, \quad (9)$$

which is the gamma distribution. The parameter  $\alpha$  in (9) is the ratio of the average variance  $\theta$  to the characteristic fluctuation of variance  $\kappa^2/2\gamma$  during the relaxation time  $1/\gamma$ . When  $\alpha \rightarrow \infty$ ,  $\Pi_*(v) \rightarrow \delta(v - \theta)$ . The corresponding stationary PDF of volatility  $\sigma$  is

$$\Pi_*^{(\sigma)}(\sigma) = \frac{2\alpha^\alpha}{\Gamma(\alpha)} \frac{\sigma^{2\alpha-1}}{\theta^\alpha} e^{-\alpha\sigma^2/\theta}. \quad (10)$$

Functions (9) and (10) are integrable as long as  $\alpha > 0$ . The distributions  $\Pi_*(v)$  and  $\Pi_*^{(\sigma)}(\sigma)$  are shown in figure 1 for the value  $\alpha = 1.3$  deduced from the fit of the Dow-Jones time series and given in table 1 in section 8.

### 3. Solution of the Fokker–Planck equation

Since  $x$  appears in (6) only in the derivative operator  $\partial/\partial x$ , it is convenient to take the Fourier transform

$$P_t(x, v|v_i) = \int_{-\infty}^{+\infty} \frac{dp_x}{2\pi} e^{ip_x x} \bar{P}_{t,p_x}(v|v_i). \quad (11)$$

Inserting (11) into (6), we find

$$\begin{aligned} \frac{\partial}{\partial t} \bar{P} &= \gamma \frac{\partial}{\partial v} [(v - \theta) \bar{P}] \\ &- \left[ \frac{p_x^2 - ip_x}{2} v - i\rho\kappa p_x \frac{\partial}{\partial v} v - \frac{\kappa^2}{2} \frac{\partial^2}{\partial v^2} v \right] \bar{P}. \end{aligned} \quad (12)$$

Equation (12) is simpler than (6), because the number of variables has been reduced to two,  $v$  and  $t$ , whereas  $p_x$  only plays the role of a parameter.

Since equation (12) is linear in  $v$  and quadratic in  $\partial/\partial v$ , it can be simplified by taking the Laplace transform over  $v$

$$\tilde{P}_{t,p_x}(p_v|v_i) = \int_0^{+\infty} dv e^{-p_v v} \bar{P}_{t,p_x}(v|v_i). \quad (13)$$

The partial differential equation satisfied by  $\tilde{P}_{t,p_x}(p_v|v_i)$  is of the first order

$$\left[ \frac{\partial}{\partial t} + \left( \Gamma p_v + \frac{\kappa^2}{2} p_v^2 - \frac{p_x^2 - ip_x}{2} \right) \frac{\partial}{\partial p_v} \right] \tilde{P} = -\gamma\theta p_v \tilde{P}, \quad (14)$$

where we introduced the notation

$$\Gamma = \gamma + i\rho\kappa p_x. \quad (15)$$

Equation (14) has to be solved with the initial condition

$$\tilde{P}_{t=0,p_x}(p_v|v_i) = \exp(-p_v v_i). \quad (16)$$

The solution of (14) is given by the method of characteristics [20]:

$$\tilde{P}_{t,p_x}(p_v|v_i) = \exp\left(-\tilde{p}_v(0)v_i - \gamma\theta \int_0^t d\tau \tilde{p}_v(\tau)\right), \quad (17)$$

where the function  $\tilde{p}_v(\tau)$  is the solution of the characteristic (ordinary) differential equation

$$\frac{d\tilde{p}_v(\tau)}{d\tau} = \Gamma \tilde{p}_v(\tau) + \frac{\kappa^2}{2} \tilde{p}_v^2(\tau) - \frac{p_x^2 - ip_x}{2} \quad (18)$$

with the boundary condition  $\tilde{p}_v(t) = p_v$  specified at  $\tau = t$ . The differential equation (18) is of the Riccati type with constant coefficients [21], and its solution is

$$\tilde{p}_v(\tau) = \frac{2\Omega}{\kappa^2} \frac{1}{\zeta e^{\Omega(t-\tau)} - 1} - \frac{\Gamma - \Omega}{\kappa^2}, \quad (19)$$

where we introduced the frequency

$$\Omega = \sqrt{\Gamma^2 + \kappa^2(p_x^2 - ip_x)} \quad (20)$$

and the coefficient

$$\zeta = 1 + \frac{2\Omega}{\kappa^2 p_x + (\Gamma - \Omega)}. \quad (21)$$

Substituting (19) into (17), we find

$$\begin{aligned} \tilde{P}_{t,p_x}(p_v|v_i) &= \exp\left\{-\tilde{p}_v(0)v_i + \frac{\gamma\theta(\Gamma - \Omega)t}{\kappa^2} - \frac{2\gamma\theta}{\kappa^2} \ln \frac{\zeta - e^{-\Omega t}}{\zeta - 1}\right\}. \end{aligned} \quad (22)$$

## 4. Averaging over variance

Normally we are interested only in log-returns  $x$  and do not care about variance  $v$ . Moreover, whereas log-returns are directly known from financial data, variance is a hidden stochastic variable that has to be estimated. Inevitably, such an estimation is done with some degree of uncertainty, which precludes a clear-cut direct comparison between  $P_t(x, v|v_i)$  and financial data. Thus we introduce the reduced probability distribution

$$P_t(x|v_i) = \int_0^{+\infty} dv P_t(x, v|v_i) = \int \frac{dp_x}{2\pi} e^{ip_x x} \tilde{P}_{t,p_x}(0|v_i), \quad (23)$$

where the hidden variable  $v$  is integrated out, so  $p_v = 0$ . Substituting  $\zeta$  from (21) with  $p_v = 0$  into (22), we find

$$\begin{aligned} P_t(x|v_i) &= \int_{-\infty}^{+\infty} \frac{dp_x}{2\pi} \exp\left(ip_x x - v_i \frac{p_x^2 - ip_x}{\Gamma + \Omega \coth(\Omega t/2)}\right) \\ &\times \exp\left(-\frac{2\gamma\theta}{\kappa^2} \ln\left(\cosh \frac{\Omega t}{2} + \frac{\Gamma}{\Omega} \sinh \frac{\Omega t}{2}\right) + \frac{\gamma\Gamma\theta t}{\kappa^2}\right). \end{aligned} \quad (24)$$

To check the validity of (24), let us consider the limiting case  $\kappa = 0$ . In this case, the stochastic term in (2) is absent, so the time evolution of variance is deterministic:

$$v_t = \theta + (v_i - \theta)e^{-\gamma t}. \quad (25)$$

Then process (5) gives a Gaussian distribution for  $x$ ,

$$P_t^{(\kappa=0)}(x|v_i) = \frac{1}{\sqrt{2\pi t \bar{v}_t}} \exp\left(-\frac{(x + \bar{v}_t t/2)^2}{2\bar{v}_t t}\right), \quad (26)$$

with the time-averaged variance  $\bar{v}_t = \frac{1}{t} \int_0^t d\tau v_\tau$ . On the other hand, by taking the limit  $\kappa \rightarrow 0$  and integrating over  $p_x$  in (24), we reproduce the same expression (26).

Equation (24) cannot be directly compared with financial time series data, because it depends on the unknown initial variance  $v_i$ . In order to resolve this problem, we assume that  $v_i$  has the stationary probability distribution  $\Pi_*(v_i)$ , which is given by (9). Thus we introduce the PDF  $P_t(x)$  by averaging (24) over  $v_i$  with the weight  $\Pi_*(v_i)$ :

$$P_t(x) = \int_0^\infty dv_i \Pi_*(v_i) P_t(x|v_i). \quad (27)$$

The integral over  $v_i$  is similar to the one of the gamma function and can be taken explicitly. The final result is the Fourier integral

$$P_t(x) = \frac{1}{2\pi} \int_{-\infty}^{+\infty} dp_x e^{ip_x x + F_t(p_x)} \quad (28)$$

with

$$\begin{aligned} F_t(p_x) &= \frac{\gamma\theta}{\kappa^2} \Gamma t \\ &- \frac{2\gamma\theta}{\kappa^2} \ln\left[\cosh \frac{\Omega t}{2} + \frac{\Omega^2 - \Gamma^2 + 2\gamma\Gamma}{2\gamma\Omega} \sinh \frac{\Omega t}{2}\right]. \end{aligned} \quad (29)$$

The variable  $p_x$  enters (29) via the variables  $\Gamma$  from (15) and  $\Omega$  from (20). It is easy to check that  $P_t(x)$  is real, because  $\text{Re } F$  is an even function of  $p_x$  and  $\text{Im } F$  is an odd one. One

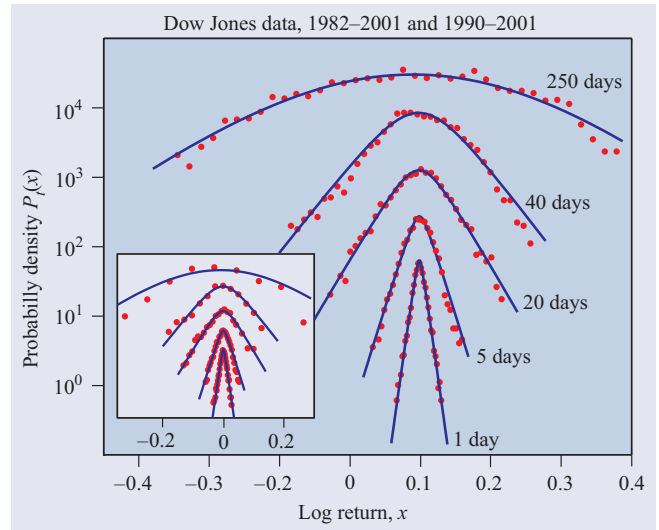


**Figure 2.** Probability distribution  $P_t(x)$  of log-return  $x$  for different time lags  $t$ . Points: the 1982–2001 Dow–Jones data for  $t = 1, 5, 20, 40$ , and 250 trading days. Solid curves: fit of the data with equations (28) and (29). For clarity, the data points and the curves for successive  $t$  are shifted up by the factor of 10 each. Inset: the 1990–2001 Dow–Jones data points compared with the same theoretical curves.

can also check that  $F_t(p_x = 0) = 0$ , which implies that  $P_t(x)$  is correctly normalized at all times:  $\int dx P_t(x) = 1$ . The simplified version of equation (29) for the case  $\rho = 0$  is given in appendix A.

Equations (28) and (29) for the probability distribution  $P_t(x)$  of log-return  $x$  at time  $t$  are the central analytical result of the paper. The integral in (28) can be calculated numerically or, in certain regimes discussed in sections 5–7, analytically. In figure 2, the calculated function  $P_t(x)$ , shown by solid curves, is compared with the Dow–Jones data, shown by dots. (Technical details of the data analysis are discussed in section 8.) Figure 2 demonstrates that, with a fixed set of the parameters  $\gamma, \theta, \kappa, \mu$ , and  $\rho$ , equations (28) and (29) very well reproduce the PDF of log-returns  $x$  of the Dow–Jones index for all times  $t$ . In the log–linear scale of figure 2, the tails of  $\ln P_t(x)$  versus  $x$  are straight lines, which means that the tails of  $P_t(x)$  are exponential in  $x$ . For short times  $t$ , the distribution is narrow, and the slopes of the tails are nearly vertical. As the time  $t$  progresses, the PDF broadens and flattens.

## 5. Asymptotic behaviour for long time $t$

Equation (2) implies that variance reverts to the equilibrium value  $\theta$  within the characteristic relaxation time  $1/\gamma$ . In this section, we consider the asymptotic limit where time  $t$  is much longer than the relaxation time:  $\gamma t \gg 2$ . According to (15) and (20), this condition also implies that  $\Omega t \gg 2$ . Then equation (29) reduces to

$$F_t(p_x) \approx \frac{\gamma\theta t}{\kappa^2} (\Gamma - \Omega). \quad (30)$$

Let us change the variable of integration in (28) to

$$p_x = \frac{\omega_0}{\kappa\sqrt{1-\rho^2}}\tilde{p}_x + i p_0, \quad (31)$$

where

$$p_0 = \frac{\kappa - 2\rho\gamma}{2\kappa(1-\rho^2)}, \quad \omega_0 = \sqrt{\gamma^2 + \kappa^2(1-\rho^2)p_0^2}. \quad (32)$$

Substituting (31) into (15), (20), and (30), we transform (28) to the following form:

$$P_t(x) = \frac{\omega_0 e^{-p_0 x + \Lambda t}}{\pi\kappa\sqrt{1-\rho^2}} \int_0^\infty d\tilde{p}_x \cos(A\tilde{p}_x) e^{-B\sqrt{1+\tilde{p}_x^2}}, \quad (33)$$

where

$$A = \frac{\omega_0}{\kappa\sqrt{1-\rho^2}} \left( x + \rho \frac{\gamma\theta t}{\kappa} \right), \quad B = \frac{\gamma\theta\omega_0 t}{\kappa^2}, \quad (34)$$

and

$$\Lambda = \frac{\gamma\theta}{2\kappa^2} \frac{2\gamma - \rho\kappa}{1 - \rho^2}. \quad (35)$$

According to formula 3.914 from [22], the integral in (33) is equal to  $B K_1(\sqrt{A^2 + B^2})/\sqrt{A^2 + B^2}$ , where  $K_1$  is the first-order modified Bessel function.

Thus, equation (28) in the limit  $\gamma t \gg 2$  can be represented in the scaling form

$$P_t(x) = N_t e^{-p_0 x} P_*(z), \quad P_*(z) = K_1(z)/z, \quad (36)$$

where the argument  $z = \sqrt{A^2 + B^2}$  is

$$z = \frac{\omega_0}{\kappa} \sqrt{\frac{(x + \rho\gamma\theta t/\kappa)^2}{1 - \rho^2} + \left(\frac{\gamma\theta t}{\kappa}\right)^2}, \quad (37)$$

and the time-dependent normalization factor  $N_t$  is

$$N_t = \frac{\omega_0^2 \gamma \theta t}{\pi \kappa^3 \sqrt{1 - \rho^2}} e^{\Lambda t}. \quad (38)$$

Equation (36) demonstrates that, up to the factors  $N_t$  and  $e^{-p_0 x}$ , the dependence of  $P_t(x)$  on the two arguments  $x$  and  $t$  is given by the function  $P_*(z)$  of the single scaling argument  $z$  in (37). Thus, when plotted as a function of  $z$ , the data for different  $x$  and  $t$  should collapse on the single universal curve  $P_*(z)$ . This is beautifully illustrated by figure 3, where the Dow-Jones data for different time lags  $t$  follow the curve  $P_*(z)$  for seven orders of magnitude.

In the limit  $z \gg 1$ , we can use the asymptotic expression [22]  $K_1(z) \approx e^{-z} \sqrt{\pi/2z}$  in (36) and take the logarithm of  $P$ . Keeping only the leading term proportional to  $z$  and omitting the subleading term proportional to  $\ln z$ , we find that  $\ln P_t(x)$  has the hyperbolic distribution [2, p 14]

$$\ln \frac{P_t(x)}{N_t} \approx -p_0 x - z \quad \text{for } z \gg 1. \quad (39)$$

Let us examine equation (39) for large and small  $|x|$ .

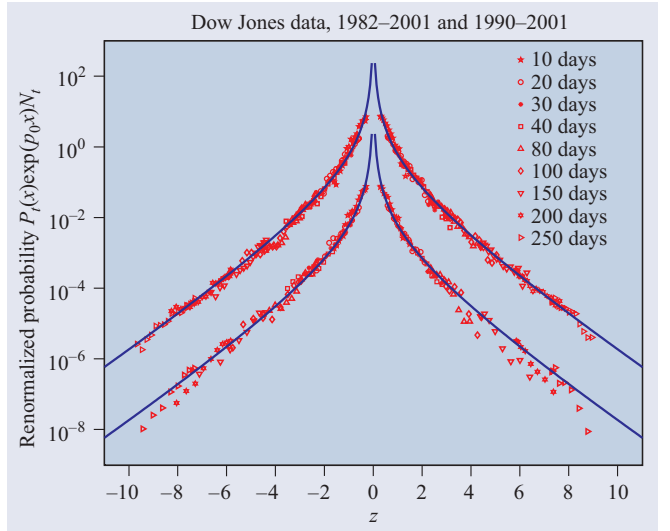


**Figure 3.** Renormalized probability density  $P_t(x)e^{p_0 x}/N_t$  plotted as a function of the scaling argument  $z$  given by (37). Solid curves: the scaling function  $P_*(z) = K_1(z)/z$  from (36), where  $K_1$  is the first-order modified Bessel function. Upper and lower sets of points: the 1982–2001 and 1990–2001 Dow–Jones data for different time lags  $t$ . For clarity, the lower data set and the curve are shifted by the factor of  $10^{-2}$ .

In the first case  $|x| \gg \gamma\theta t/\kappa$ , equation (37) gives  $z \approx \omega_0|x|/\kappa\sqrt{1-\rho^2}$ , so equation (39) becomes

$$\ln \frac{P_t(x)}{N_t} \approx -p_0 x - \frac{\omega_0}{\kappa\sqrt{1-\rho^2}}|x|. \quad (40)$$

Thus, the PDF  $P_t(x)$  has the exponential tails (40) for large log-returns  $|x|$ . Notice that, in the considered limit  $\gamma t \gg 2$ , the slopes  $d \ln P/dx$  of the exponential tails (40) do not depend on time  $t$ . Because of  $p_0$ , the slopes (40) for positive and negative  $x$  are not equal, thus the distribution  $P_t(x)$  is not symmetric with respect to positive and negative price changes. According to (32), this asymmetry is enhanced by a negative correlation  $\rho < 0$  between stock price and variance.

In the second case  $|x + \rho\gamma\theta t/\kappa| \ll \gamma\theta t/\kappa$ , by Taylor-expanding  $z$  in (37) near its minimum in  $x$  and substituting the result into (39), we get

$$\ln \frac{P_t(x)}{N'_t} \approx -p_0 x - \frac{\omega_0(x + \rho\gamma\theta t/\kappa)^2}{2(1-\rho^2)\gamma\theta t}, \quad (41)$$

where  $N'_t = N_t \exp(-\omega_0\gamma\theta t/\kappa^2)$ . Thus, for small log-returns  $|x|$ , the PDF  $P_t(x)$  is Gaussian with the width increasing linearly in time. The maximum of  $P_t(x)$  in (41) is achieved at

$$x_m(t) = -\frac{\gamma\theta t}{2\omega_0} \left( 1 + 2\frac{\rho(\omega_0 - \gamma)}{\kappa} \right). \quad (42)$$

Equation (42) gives the most probable log-return  $x_m(t)$  at time  $t$ , and the coefficient in front of  $t$  constitutes a correction to the average growth rate  $\mu$ , so that the actual growth rate is  $\bar{\mu} = \mu + dx_m/dt$ .

As figure 2 illustrates,  $\ln P_t(x)$  is indeed linear in  $x$  for large  $|x|$  and quadratic for small  $|x|$ , in agreement

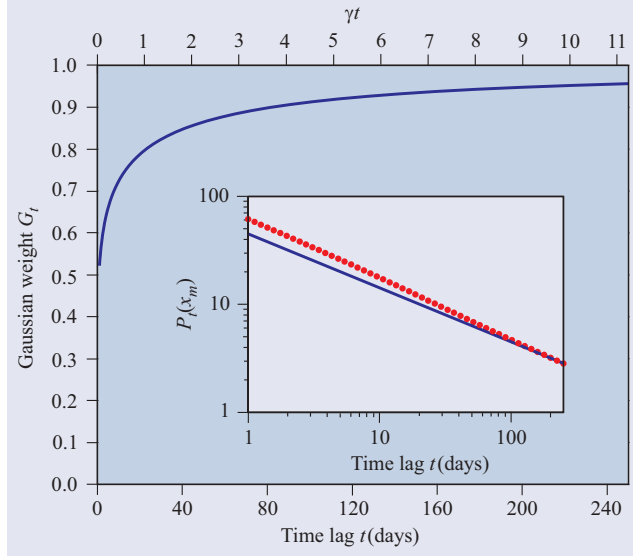


**Figure 4.** The fraction  $G_t$  of the total probability contained in the Gaussian part of  $P_t(x)$  versus time lag  $t$ . Inset: time dependence of the probability density at maximum  $P_t(x_m)$  (points), compared with the Gaussian  $t^{-1/2}$  behaviour (solid curve).

with (40) and (41). As time progresses, the distribution, which has the scaling form (36) and (37), broadens. Thus, the fraction  $G_t$  of the total probability contained in the parabolic (Gaussian) portion of the curve increases, as illustrated in figure 4. (The procedure of calculating  $G_t$  is explained in appendix B.) Figure 4 shows that, at sufficiently long times, the total probability contained in the non-Gaussian tails becomes negligible, which is known in the literature [2]. The inset in figure 4 illustrates that the time dependence of the probability density at maximum,  $P_t(x_m)$ , is close to  $t^{-1/2}$ , which is characteristic for a Gaussian evolution.

## 6. Asymptotic behaviour for large log-return $x$

In the complex plane of  $p_x$ , function  $F(p_x)$  becomes singular at the points  $p_x$  where the argument of the logarithm in (29) vanishes. These points are located on the imaginary axis of  $p_x$  and are shown by dots in figure 5. The singularity closest to the real axis is located on the positive (negative) imaginary axis at the point  $p_1^+$  ( $p_1^-$ ). Because the argument of the logarithm in (29) vanishes at these two points, we can approximate  $F(p_x)$  by the dominant, singular term:  $F(p_x) \approx -(2\gamma\theta/\kappa^2) \ln(p_x - p_1^\pm)$ .

For large  $|x|$ , the integrand of (28) oscillates very fast as a function of  $p_x$ . Thus, we can evaluate the integral using the method of stationary phase [21] by shifting the contour of integration so that it passes through a saddle point of the argument  $ip_x x + F(p_x)$  of the exponent in (28). The saddle point position  $p_s$ , shown in figure 5 by the cross, is determined

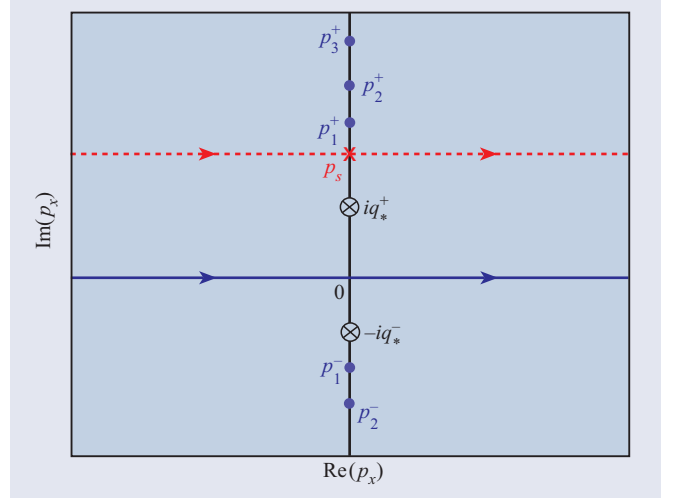


**Figure 5.** Complex plane of  $p_x$ . Dots: the singularities of  $F(p_x)$ . Circled crosses: the accumulation points  $\pm iq_*^\pm$  of the singularities in the limit  $\gamma t \gg 2$ . Cross: the saddle point  $p_s$ , which is located in the upper half-plane for  $x > 0$ . Dashed line: the contour of integration displaced from the real axis in order to pass through the saddle point  $p_s$ .

by the equation

$$ix = -\frac{dF(p_x)}{dp_x} \Big|_{p_x=p_s} \approx \frac{2\gamma\theta}{\kappa^2} \begin{cases} \frac{1}{p_s - p_1^+}, & x > 0, \\ \frac{1}{p_s - p_1^-}, & x < 0. \end{cases} \quad (43)$$

For a large  $|x|$ , such that  $|xp_x^\pm| \gg 2\gamma\theta/\kappa^2$ , the saddle point  $p_s$  is very close to the singularity point:  $p_s \approx p_1^+$  for  $x > 0$  and  $p_s \approx p_1^-$  for  $x < 0$ . Then the asymptotic expression for the probability distribution is

$$P_t(x) \sim \begin{cases} e^{-xq_1^+}, & x > 0, \\ e^{xq_1^-}, & x < 0, \end{cases} \quad (44)$$

where  $q_t^\pm = \mp ip_1^\pm(t)$  are real and positive. Equation (44) shows that, for all times  $t$ , the tails of the probability distribution  $P_t(x)$  for large  $|x|$  are exponential. The slopes of the exponential tails,  $q_t^\pm = \mp d \ln P_t(x)/dx$ , are determined by the positions  $p_1^\pm$  of the singularities closest to the real axis.

These positions  $p_1^\pm(t)$  and, thus, the slopes  $q_t^\pm$  depend on time  $t$ . For times much shorter than the relaxation time ( $\gamma t \ll 2$ ), the singularities lie far away from the real axis. As time increases, the singularities move along the imaginary axis toward the real axis. Finally, for times much longer than the relaxation time ( $\gamma t \gg 2$ ), the singularities approach limiting points:  $p_1^\pm \rightarrow \pm iq_*^\pm$ , which are shown in figure 5 by circled crosses. Thus, as illustrated in figure 6, the slopes  $q_t^\pm$  monotonically decrease in time and saturate at long times:

$$q_t^\pm \rightarrow q_*^\pm = \frac{\omega_0}{\kappa\sqrt{1-\rho^2}} \pm p_0 \quad \text{for } \gamma t \gg 2. \quad (45)$$

The slopes (45) are in agreement with equation (40) valid for  $\gamma t \gg 2$ . The time dependence  $q_t^\pm$  at short times can also be

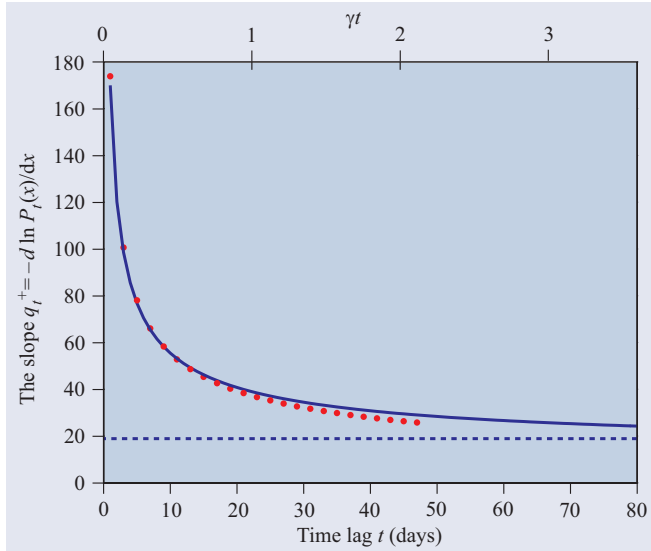


**Figure 6.** Solid curve: the slope  $q_t^+ = -d \ln P_t(x)/dx$  of the exponential tail for  $x > 0$  as a function of time. Points: the asymptotic approximation (46) for the slope in the limit  $\gamma t \ll 2$ . Dashed line: the saturation value  $q_*^+$  of  $q_t^+$  for  $\gamma t \gg 2$ , equation (45).

found analytically:

$$q_t^\pm \approx \frac{2}{\kappa} \sqrt{\frac{\gamma}{t}} \quad \text{for } \gamma t \ll 2. \quad (46)$$

The dotted curve in figure 6 shows that equation (46) works very well for short times  $t$ , where the slope diverges at  $t \rightarrow 0$ .

## 7. Asymptotic behaviour for short time $t$

For a short time  $t$ , we expand the equations of section 3 to the first order in  $t$  and set  $p_v = 0$ . The last term in equation (22) cancels the penultimate term, and equation (18) gives  $\tilde{p}_v(0) = t(p_x^2 - ip_x)/2$ . Substituting this formula into (22) and taking the integral (23) over  $p_x$ , we find

$$P_t(x|v_i) = \frac{1}{\sqrt{2\pi v_i t}} \exp\left(-\frac{(x + v_i t/2)^2}{2v_i t}\right). \quad (47)$$

Equation (47) shows that, for a short  $t$ , the probability distribution of  $x$  evolves in a Gaussian manner with the initial variance  $v_i$ , because variance has no time to change.

Substituting (47) and (9) into (27), we find

$$P_t(x) = \frac{\alpha^\alpha}{\Gamma(\alpha)} \frac{e^{-x/2}}{\sqrt{2\pi\theta t}} \int_0^\infty d\tilde{v}_i \tilde{v}_i^{C-1} e^{-A\tilde{v}_i - B/\tilde{v}_i} \quad (48)$$

where  $\tilde{v}_i = v_i/\theta$ ,  $A = \alpha + \theta t/8$ ,  $B = x^2/2\theta t$ , and  $C = \alpha - 1/2$ . According to formula 3.471.9 from [22], the integral in (48) is  $2(B/A)^{C/2} K_C(2\sqrt{AB})$  for  $\operatorname{Re} A > 0$  and  $\operatorname{Re} B > 0$ , where  $K_C$  is the modified Bessel function of the order  $C$ . Taking into account that  $A \approx \alpha$  (because  $t \ll 16\gamma/\kappa^2$  for short  $t$ ), we obtain the final expression

$$P_t(x) = \frac{2^{1-\alpha} e^{-x/2}}{\Gamma(\alpha)} \sqrt{\frac{\alpha}{\pi\theta t}} y^{\alpha-1/2} K_{\alpha-1/2}(y), \quad (49)$$

where we introduced the scaling variable

$$y = \sqrt{\frac{2\alpha x^2}{\theta t}} = \frac{2\sqrt{\gamma}}{\kappa} \frac{|x|}{\sqrt{t}}. \quad (50)$$

In the limit  $y \gg 1$ , using the formula  $K_\nu(y) \approx e^{-y} \sqrt{\pi/2y}$  in (49), we find

$$P_t(x) \approx \frac{2^{1/2-\alpha}}{\Gamma(\alpha)} \sqrt{\frac{\alpha}{\theta t}} y^{\alpha-1} e^{-y} \quad \text{for } y \gg 1. \quad (51)$$

Equations (50) and (51) show that the tails of the distribution are exponential in  $x$ , and the slopes  $d \ln P_t(x)/dx$  are in agreement with equation (46).

In the opposite limit  $y \ll 1$ , the small argument expansion of the Bessel function can be found from the following equations [23]:

$$\begin{aligned} K_\nu(y) &= \frac{\pi}{2} \frac{I_{-\nu}(y) - I_\nu(y)}{\sin(\nu\pi)}, \\ \frac{\pi}{\sin(\pi\nu)} &= \Gamma(\nu)\Gamma(1-\nu), \end{aligned} \quad (52)$$

and

$$I_\nu(y) \approx \left(\frac{y}{2}\right)^\nu \sum_{k=0}^{\infty} \frac{(y^2/4)^k}{k! \Gamma(\nu+k+1)}. \quad (53)$$

Substituting (53) into (52), we find in the case  $1/2 \leq \alpha < 3/2$

$$\begin{aligned} K_{\alpha-1/2}(y) &\approx \frac{\Gamma(\alpha-1/2)}{2} \left(\frac{y}{2}\right)^{-\alpha+1/2} \\ &+ \frac{\Gamma(-\alpha+1/2)}{2} \left(\frac{y}{2}\right)^{\alpha-1/2}. \end{aligned} \quad (54)$$

Substituting (54) into (49), we obtain

$$P_t(x) \approx \frac{\Gamma(\alpha-1/2)}{\Gamma(\alpha)} \sqrt{\frac{\alpha}{2\pi\theta t}} \left[ 1 - \lambda \left(\frac{y}{2}\right)^{2\alpha-1} \right], \quad (55)$$

where we introduced the coefficient

$$\lambda = \frac{|\Gamma(-\alpha+1/2)|}{\Gamma(\alpha-1/2)}. \quad (56)$$

Equation (55) can be written in the form

$$\ln P_t(x) - \ln P_t(0) \approx -\lambda \left(\frac{y}{2}\right)^{2\alpha-1} \quad \text{for } y \ll 1. \quad (57)$$

We see that  $\ln P_t(x)$  approaches  $x = 0$  as a power of  $x$  lower than 2 (for  $1/2 \leq \alpha < 3/2$ ). The slope  $d \ln P_t(x)/dx$  at  $x \rightarrow 0$  is zero for  $\alpha > 1$  and infinite for  $\alpha < 1$ .

## 8. Comparison with the Dow–Jones time series

To test the model against financial data, we downloaded daily closing values of the Dow–Jones industrial index for the period of 20 years from 1 January 1982 to 31 December 2001 from the web site of Yahoo [24]. The data set contains 5049 points, which form the time series  $\{S_\tau\}$ , where the integer time variable

**Table 1.** Parameters of the Heston model obtained from the fit of the Dow–Jones data using  $\rho = 0$  for the correlation coefficient. We also find  $1/\gamma = 22.2$  trading days for the relaxation time of variance,  $\alpha = 2\gamma\theta/\kappa^2 = 1.3$  for the parameter in the variance distribution function (9), and  $x_0 = \kappa/\gamma = 5.4\%$  for the characteristic scale (A.4) of  $x$ .

Units	$\gamma$	$\theta$	$\kappa$	$\mu$
1/day	$4.50 \times 10^{-2}$	$8.62 \times 10^{-5}$	$2.45 \times 10^{-3}$	$5.67 \times 10^{-4}$
1/year	11.35	0.022	0.618	0.143

$\tau$  is the trading day number. We do not filter the data for short days, such as those before holidays.

Given  $\{S_\tau\}$ , we use the following procedure to extract the probability density  $P_t^{(DJ)}(r)$  of log-return  $r$  for a given time lag  $t$ . For fixed  $t$ , we calculate the set of log-returns  $\{r_\tau = \ln S_{\tau+t}/S_\tau\}$  for all possible times  $\tau$ . Then we partition the  $r$ -axis into equally spaced bins of width  $\Delta r$  and count the number of log-returns  $r_\tau$  belonging to each bin. In this process, we omit the bins with occupation numbers less than five, because we consider such small statistics unreliable. Only less than 1% of the entire data set is omitted in this procedure. Dividing the occupation number of each bin by  $\Delta r$  and by the total occupation number of all bins, we obtain the probability density  $P_t^{(DJ)}(r)$  for a given time lag  $t$ . To find  $P_t^{(DJ)}(x)$ , we replace  $r \rightarrow x + \mu t$ .

Assuming that the system is ergodic, so that ensemble averaging is equivalent to time averaging, we compare  $P_t^{(DJ)}(x)$  extracted from the time series data and  $P_t(x)$  calculated in previous sections, which describes ensemble distribution. In the language of mathematical statistics, we compare our theoretically derived population distribution with the sample distribution extracted from the time series data. We determine parameters of the model by minimizing the mean-square deviation  $\sum_{x,t} |\ln P_t^{(DJ)}(x) - \ln P_t(x)|^2$ , where the sum is taken over all available  $x$  and  $t = 1, 5, 20, 40$ , and 250 days. These values of  $t$  are selected because they represent different regimes:  $\gamma t \ll 1$  for  $t = 1$  and 5 days,  $\gamma t \approx 1$  for  $t = 20$  days, and  $\gamma t \gg 1$  for  $t = 40$  and 250 days. As figures 2 and 3 illustrate, our expression (28) and (29) for the probability density  $P_t(x)$  agrees with the data very well, not only for the selected five values of time  $t$ , but for the whole time interval from 1 to 250 trading days. However, we cannot extend this comparison to  $t$  longer than 250 days, which is approximately 1/20 of the entire range of the data set, because we cannot reliably extract  $P_t^{(DJ)}(x)$  from the data when  $t$  is too long.

The values obtained for the four fitting parameters ( $\gamma, \theta, \kappa, \mu$ ) are given in table 1. We find that our fits are not very sensitive to the value of  $\rho$ , so we cannot reliably determine it. Thus, we use  $\rho = 0$  for simplicity, which gives a good fit of the data. On the other hand, a nonzero value of  $\rho$  was found in [25] by fitting the leverage correlation function introduced in [26] and [13–15] by fitting the option prices.

All four parameters ( $\gamma, \theta, \kappa, \mu$ ) shown in table 1 have the dimensionality of 1/time. The first line of the table gives their values in units of 1/day, as originally determined in our fit. The second line shows the annualized values of the parameters in units of 1/year, where we utilize the average number of 252.5 trading days per calendar year to make the conversion. The relaxation time of variance is equal to  $1/\gamma = 22.2$  trading days = 4.4 weeks  $\approx$  1 month, where we took into account that

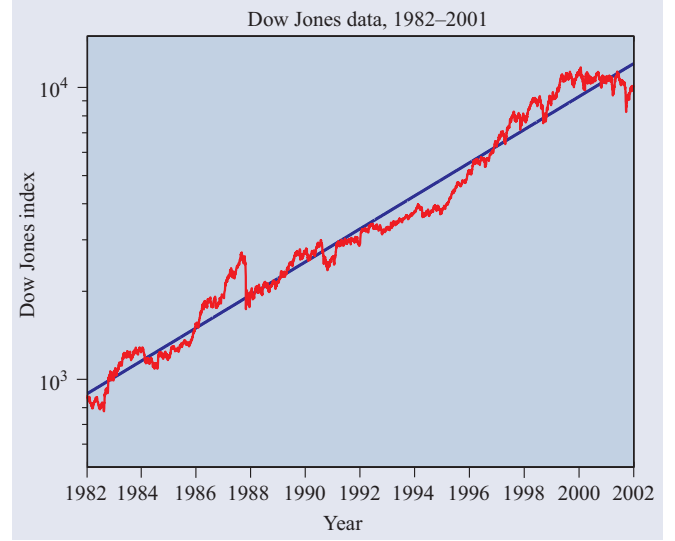


**Figure 7.** Time dependence of the Dow–Jones index shown on a log–linear scale. The straight line represents the average exponential growth in time.

1 week = 5 trading days. Thus, we find that variance has a rather long relaxation time, of the order of one month, which is in agreement with the conclusion of [25].

The effective growth rate of stock prices is determined by the coordinate  $r_m(t)$  where the probability density  $P_t(r_m)$  is maximal. Using the relation  $r_m = x_m + \mu t$  and equation (42), we find that the actual growth rate is  $\bar{\mu} = \mu - \gamma\theta/2\omega_0 \approx \mu - \theta/2 = 13\%/\text{year}$ . (Here we took into account that  $\omega_0 \approx \gamma$ , because  $\gamma \gg \kappa/2$  in equation (32).) This number coincides with the average growth rate of the Dow–Jones index obtained by a simple fit of the time series  $\{S_\tau\}$  with an exponential function of  $\tau$ , as shown in figure 7. The effective stock growth rate  $\bar{\mu}$  is comparable with the average stock volatility after one year  $\sigma = \sqrt{\theta} = 14.7\%$ . Moreover, as figure 1 shows, the distribution of variance is broad, and the variation of variance is comparable to its average value  $\theta$ . Thus, even though the average growth rate of the stock index is positive, there is a substantial probability  $\int_{-\infty}^0 dr P_t(r) = 17.7\%$  of having a negative return for  $t = 1$  year.

According to (45), the asymmetry between the slopes of exponential tails for positive and negative  $x$  is given by the parameter  $p_0$ , which is equal to 1/2 when  $\rho = 0$  (see also the discussion of equation (A.1) in appendix A). The origin of this asymmetry can be traced back to the transformation from (1) to (4) using Itô's formula. It produces the term  $0.5v_t dt$  in the rhs of (4), which then generates the second term in the rhs of (6). The latter term is the only source of asymmetry in  $x$  of  $P_t(x)$  when  $\rho = 0$ . However, in practice, the asymmetry

of the slopes  $p_0 = 1/2$  is quite small (about 2.7%) compared with the average slope  $q_*^\pm \approx \omega_0/\kappa \approx 1/x_0 = 18.4$ .

By fitting the Dow–Jones data to our formula, we implicitly assumed that the parameters of the stochastic process  $(\gamma, \theta, \kappa, \mu)$  do not change in time. While this assumption may be reasonable for a limited time interval, the parameters generally could change in time. The time interval of our fit, 1982–2001, includes the crash of 1987, so one might expect that the parameters of the fit would change if we use a different interval. To verify this conjecture, in figures 2 and 3, we also compare the data points for the time interval 1990–2001 with the theoretical curves produced using the same values for the parameters as shown in table 1. Although the empirical data points in the tails for long time lags decrease somewhat faster than the theory predicts, the overall agreement is quite reasonable. We find that changing the values of the fitting parameters does not visibly improve the agreement. Thus, we conclude that the parameters of the Heston stochastic process are essentially the same for the 1980s and 1990s. Apparently, the crash of 1987 produced little effect on the probability distribution of returns, because the stock market quickly resumed its overall growth. On the other hand, our study [35] indicates that the data for the 2000s do not follow our theoretical curves with the same fitting parameters. The main difference appears to be in the average growth rate  $\mu$ , which became negative in the 2000s, as opposed to +13%/year in the 1980s and 1990s. Unfortunately, the statistics for the 2000s is limited, because we have only a few years. Nevertheless, it does seem to indicate that in the 2000s the stock market switched to a different regime compared with the 1980s and 1990s.

## 9. Discussion and conclusions

We derived an analytical solution for the PDF  $P_t(x)$  of log-returns  $x$  as a function of time lag  $t$  for the Heston model of a geometrical Brownian motion with stochastic variance. The final result has the form of a one-dimensional Fourier integral (28) and (29). (In the case  $\rho = 0$ , the equations have the simpler form presented in appendix A.) Our result agrees very well with the Dow–Jones data, as shown in figure 2. Comparing the theory and the data, we determine the four (non-zero) fitting parameters of the model, particularly the variance relaxation time  $1/\gamma = 22.2$  days. For time longer than  $1/\gamma$ , our theory predicts the scaling behaviour (36) and (37), which the Dow–Jones data indeed exhibit over seven orders of magnitude, as shown in figure 3. The scaling function  $P_*(z) = K_1(z)/z$  is expressed in terms of the first-order modified Bessel function  $K_1$ . Previous estimates in the literature of the relaxation time of volatility using various indirect indicators range from 1.5 [8, p 80] to 73 days for the half-life of the Dow–Jones index [7]. Since we have a good fit of the entire family of PDFs for time lags from 1 to 250 trading days, we believe that our estimate, 22.2 days, is more reliable. A close value of 19.6 days was found in [25].

An alternative point of view in the literature is that the time evolution of volatility is not characterized by a single relaxation rate. As shown in appendix C, the variance correlation function

$C_t^{(v)}$  (C.4) in the Heston model has a simple exponential decay in time. However, the analysis of financial data [2, p 70] indicates that the correlation function has a power-law dependence or superposition of two (or more) exponentials with relaxation times of less than one day and more than a few tens of days. (A large amount of noise in the data makes it difficult to give a precise statement.) Reference [27] argues that volatility relaxation is multifractal and has no characteristic time. However, one should keep in mind that the total range (C.2) of variation of  $C_t^{(v)}$  is only about 77% of its saturation value, not many orders of magnitude. As figures 2 of [28] and [27] show, the main drop of  $C_t^{(v)}$  takes place within a reasonably well-defined and relatively short time, whereas residual relaxation is stretched over a very long time. In this situation, a simple exponential time dependence, while not exact, may account for the main part of relaxation and give a reasonable approximation for the purposes of our study. Alternatively, it is possible to generalize the Heston model by incorporating more than one relaxation time [14].

As figure 2 shows, the probability distribution  $P_t(x)$  is exponential in  $x$  for large  $|x|$ , where it is characterized by the time-dependent slopes  $d \ln P/dx$ . The theoretical analysis presented in section 6 shows that the slopes are determined by the singularities of the function  $F_t(p_x)$  from (29) in the complex plane of  $p_x$  that are closest to the real axis. The calculated time dependence of the slopes  $d \ln P/dx$ , shown in figure 6, agrees with the data very well, which further supports our statement that  $1/\gamma = 22.2$  days. Exponential tails in the probability distribution of stock log-returns have been noticed in literature before [2, p 61], [29]. However, time dependence of the slopes has not been recognized and analysed theoretically. As shown in figure 2, our equations give the parabolic dependence of  $\ln P_t(x)$  on  $x$  for small  $x$  and linear dependence for large  $x$ , in agreement with the data. Qualitatively similar results were found in [30] for a different model with stochastic volatility and in agreement with the NYSE index daily data. It suggests that the linear and parabolic behaviour is a generic feature of the models with stochastic volatility. In [6], the power-law dependence on  $x$  of the tails of  $P_t(x)$  was emphasized. However, the data for S&P 500 were analysed in [6] only for short time lags  $t$ , typically shorter than one day. On the other hand, our data analysis is performed for time lags longer than one day, so the results cannot be directly compared.

Deriving  $P_t(x)$  in section 4, we assumed that variance  $v$  has the stationary gamma-distribution  $\Pi_*(v)$  (9). This assumption should be compared with the data. There have been numerous attempts in the literature to reconstruct the probability distribution of volatility from the time series data [31, 32]. Generally, these papers agree that the central part of the distribution is well described by a log-normal distribution, but opinions vary on the fitting of the tails. Particularly, [32] performed a fit with an alternative probability distribution of volatility described in [2, p 88]. Unfortunately, none of these papers attempted to fit the data using equation (10), so we do not have a quantitative comparison. Taking into account that we only need the integral (27), the exact shape of  $\Pi_*(v)$  may not be so important,

and equation (9) may give a reasonably good approximation for our purposes, even if it does not fit the tails very precisely.

Although we tested our model for the Dow–Jones index, there is nothing specific in the model which indicates that it applies only to stock market data. It would be interesting to see how the model performs when applied to other time series, for example, the foreign exchange data [33], which also seem to exhibit exponential tails. Study [35] indicates that our  $P_t(x)$  also works very well for the S&P 500 and Nasdaq indices for the 1980s and 1990s. However, in the 2000s the average growth rate  $\mu$  of the stock market changed to a negative value, which complicates separation of fluctuations from the overall trend.

## Acknowledgments

We thank J-P Bouchaud and R E Prange for detailed discussions of the paper and numerous valuable comments, and A T Zheleznyak and A C Silva for careful reading of the manuscript and finding minor errors.

## Appendix A. The case $\rho = 0$

As explained in section 8, we fit the data using  $\rho = 0$  for simplicity. In this case, by shifting the variable of integration in (28)  $p_x \rightarrow p_x + i/2$ , we find

$$P_t(x) = e^{-x/2} \int_{-\infty}^{+\infty} \frac{dp_x}{2\pi} e^{ip_x x + F_t(p_x)}, \quad (\text{A.1})$$

where  $\alpha = 2\gamma\theta/\kappa^2$ ,

$$F_t(p_x) = \frac{\alpha\gamma t}{2} - \alpha \ln \left[ \cosh \frac{\Omega t}{2} + \frac{\Omega^2 + \gamma^2}{2\gamma\Omega} \sinh \frac{\Omega t}{2} \right], \quad (\text{A.2})$$

and

$$\Omega = \sqrt{\gamma^2 + \kappa^2(p_x^2 + 1/4)} \approx \gamma \sqrt{1 + p_x^2(\kappa^2/\gamma^2)}. \quad (\text{A.3})$$

Now the function  $F_t(p_x)$  is real and symmetric:  $F_t(p_x) = F_t(-p_x)$ . Thus, the integral in (A.1) is a symmetric function of  $x$ , and the only source of asymmetry of  $P_t(x)$  in  $x$  is the exponential prefactor in (A.1), as discussed at the end of section 8.

In the second equation (A.3), we took into account that, according to the values shown in table 1,  $\kappa^2/4\gamma^2 \ll 1$ . Introducing the dimensionless variables

$$\tilde{t} = \gamma t, \quad \tilde{x} = x/x_0, \quad \tilde{p}_x = p_x x_0, \quad x_0 = \kappa/\gamma, \quad (\text{A.4})$$

equations (A.1)–(A.3) can be rewritten as follows:

$$P_t(x) = \frac{e^{-x/2}}{x_0} \int_{-\infty}^{+\infty} \frac{d\tilde{p}_x}{2\pi} e^{i\tilde{p}_x \tilde{x} + F_t(\tilde{p}_x)}, \quad (\text{A.5})$$

where  $\tilde{\Omega} = \sqrt{1 + \tilde{p}_x^2}$  and

$$F_t(\tilde{p}_x) = \frac{\alpha\tilde{t}}{2} - \alpha \ln \left[ \cosh \frac{\tilde{\Omega}\tilde{t}}{2} + \frac{\tilde{\Omega}^2 + 1}{2\tilde{\Omega}} \sinh \frac{\tilde{\Omega}\tilde{t}}{2} \right]. \quad (\text{A.6})$$

It is clear from (A.4)–(A.6) that the parameter  $\alpha$  determines the shape of the function  $P_t(x)$ , whereas  $1/\gamma$  and  $x_0$  set the scales of  $t$  and  $x$ .

In the limit  $\tilde{t} \gg 2$ , the scaling function (36) for  $\rho = 0$  can be written as

$$P_t(x) = N_t e^{-x/2} K_1(z)/z, \quad z = \sqrt{\tilde{x}^2 + \tilde{t}^2}, \quad (\text{A.7})$$

where  $\tilde{t} = \alpha\tilde{t}/2 = t\theta/x_0^2$  and  $N_t = \tilde{t}e^{\tilde{t}}/\pi x_0$ . Notice that equation (A.7) has only two fitting parameters,  $x_0$  and  $\theta$ , whereas the general formula (A.5) and (A.6) has three fitting parameters. As follows from (39), for  $\tilde{x} \gg \tilde{t}$  and  $\tilde{x} \gg 1$ ,  $P_t(x) \propto \exp(-|x|/x_0)$ , so  $1/x_0$  is the slope of the exponential tails in  $x$ .

## Appendix B. Gaussian weight

Let us expand the integral in (A.1) for small  $x$ :

$$P_t(x) \approx e^{-x/2} (\mu_0 - \frac{1}{2}\mu_2 x^2), \quad (\text{B.1})$$

where the coefficients are the first and the second moments of  $\exp[F_t(p_x)]$

$$\mu_0(t) = \int_{-\infty}^{+\infty} \frac{dp_x}{2\pi} e^{F_t(p_x)}, \quad \mu_2(t) = \int_{-\infty}^{+\infty} \frac{dp_x}{2\pi} p_x^2 e^{F_t(p_x)}. \quad (\text{B.2})$$

On the other hand, we know that  $P_t(x)$  is Gaussian for small  $x$ . So, we can write

$$P_t(x) \approx \mu_0 e^{-x/2} e^{-\mu_2 x^2/2\mu_0}, \quad (\text{B.3})$$

with the same coefficients as in (B.1). If we ignore the existence of fat tails and extrapolate (B.3) to  $x \in (-\infty, \infty)$ , the total probability contained in such a Gaussian extrapolation will be

$$G_t = \int_{-\infty}^{+\infty} dx \mu_0 e^{-x/2 - \mu_2 x^2/2\mu_0} = \sqrt{\frac{2\pi\mu_0^3}{\mu_2}} e^{\mu_0/8\mu_2}. \quad (\text{B.4})$$

Obviously,  $G_t < 1$ , because the integral (B.4) does not take into account the probability contained in the fat tails. Thus, the difference  $1 - G_t$  can be taken as a measure of how much the actual distribution  $P_t(x)$  deviates from a Gaussian function.

We calculated the moments (B.2) numerically for the function  $F$  given by (A.2), then determined the Gaussian weight  $G_t$  from (B.4) and plotted it in figure 4 as a function of time. For  $t \rightarrow \infty$ ,  $G_t \rightarrow 1$ , i.e.  $P_t(x)$  becomes Gaussian for very long time lags, which is known in the literature [2]. In the opposite limit  $t \rightarrow 0$ ,  $F_t(p_x)$  becomes a very broad function of  $p_x$ , so we cannot calculate the moments  $\mu_0$  and  $\mu_2$  numerically. The singular limit  $t \rightarrow 0$  is studied analytically in section 7.

## Appendix C. Correlation function of variance

The correlation function of variance is defined as

$$C_t^{(v)} = \langle v_{t+\tau} v_\tau \rangle = \int_0^\infty dv_i \int_0^\infty dv v \Pi_t(v|v_i) v_i \Pi_*(v_i). \quad (\text{C.1})$$

It depends only on the relative time  $t$  and does not depend on the initial time  $\tau$ . The averaging  $\langle \dots \rangle$  is performed over the ensemble probability distribution, as written in (C.1), or over the initial time  $\tau$  for time series data. Equation (C.1) has the same structure as in the influence-functional formalism of Feynman and Vernon [34], where  $\Pi_r(v|v_i)$  represents the conditional probability propagator from the initial value  $v_i$  to the final value  $v$  over the time  $t$ , and  $\Pi_*(v_i)$  represents the stationary, equilibrium probability distribution of  $v_i$ .

Using equations (C.1) and (9), it is easy to find the limiting values of  $C_t^{(v)}$ :

$$\begin{aligned} C_\infty^{(v)} &= \langle v \rangle^2 = \theta^2, \\ C_0^{(v)} &= \langle v^2 \rangle = \theta^2 \left(1 + \frac{1}{\alpha}\right) = \theta^2(1 + 0.77), \end{aligned} \quad (\text{C.2})$$

where we used the numerical value from table 1.

Differentiating equation (C.1) with respect to  $t$  and using equation (8), we find that  $C_t^{(v)}$  satisfies the following differential equation:

$$\frac{dC_t^{(v)}}{dt} = -\gamma(C_t^{(v)} - \theta^2). \quad (\text{C.3})$$

Thus,  $C_t^{(v)}$  changes in time exponentially with the relaxation rate  $\gamma$ :

$$C_t^{(v)} = \theta^2 \left(1 + \frac{e^{-\gamma t}}{\alpha}\right). \quad (\text{C.4})$$

## References

- [1] Wilmott P 1998 *Derivatives* (New York: Wiley)
- [2] Bouchaud J-P and Potters M 2001 *Theory of Financial Risks* (Cambridge: Cambridge University Press)
- [3] Mantegna R N and Stanley H E 2000 *An Introduction to Econophysics* (Cambridge: Cambridge University Press)
- [4] Voit J 2001 *The Statistical Mechanics of Financial Markets* (Berlin: Springer)
- [5] Mandelbrot B B 1963 *J. Business* **36** 393
- [6] Mantegna R N and Stanley H E 1995 *Nature* **376** 46  
Gopikrishnan P, Meyer M, Amaral L A N and Stanley H E 1998 *Eur. Phys. J. B* **3** 139  
Gopikrishnan P, Plerou V, Amaral L A N, Meyer M and Stanley H E 1999 *Phys. Rev. E* **60** 5305
- [7] Engle R F and Patton A J 2001 *Quant. Finance* **1** 237
- [8] Fouque J P, Papanicolaou G and Sircar K R 2000 *Derivatives in Financial Markets with Stochastic Volatility* (Cambridge: Cambridge University Press)
- [9] Hull J and White A 1987 *J. Finance* **42** 281
- [10] Ball C A and Roma A 1994 *J. Financial Quant. Anal.* **29** 589
- [11] Schöbel R and Zhu J 1999 *Eur. Finance Rev.* **3** 23
- [12] Stein E M and Stein J C 1991 *Rev. Financial Studies* **4** 727
- [13] Heston S L 1993 *Rev. Financial Studies* **6** 327
- [14] Baaquie B E 1997 *J. Physique I* **7** 1733
- [15] Bakshi G, Cao C and Singleton K 1997 *J. Finance* **52** 2002
- [16] Duffie D, Pan J and Singleton K 2000 *Econometrica* **68** 1343
- [17] Pan J 2002 *J. Financial Economics* **63** 3
- [18] Feller W 1951 *Ann. Math.* **54** 173
- [19] McMillan D G 2001 *Appl. Econ. Lett.* **8** 605
- [20] Tompkins R G 2001 *J. Futures Markets* **21** 43  
Lin Y-N, Strong N and Xu X 2001 *J. Futures Markets* **21** 197
- [21] Fiorentini G, Leon A and Rubio G 2002 *J. Empirical Finance* **9** 225
- [22] Gardiner C W 1993 *Handbook of Stochastic Methods for Physics, Chemistry, and the Natural Sciences* (Berlin: Springer)
- [23] Courant R and Hilbert D 1962 *Methods of Mathematical Physics* vol 2 (New York: Wiley)
- [24] Bender C M and Orszag S A 1999 *Advanced Mathematical Methods for Scientists and Engineers* (New York: Springer)
- [25] Gradshteyn I S and Ryzhik I R 1996 *Table of Integrals, Series, and Products* (New York: Academic)
- [26] Abramowitz M and Stegun I A 1972 *Handbook of Mathematical Functions* (New York: Dover) p 375
- [27] Yahoo Finance <http://finance.yahoo.com/>. To download data, type in the symbol box: ‘DJI’, and then click on the link: ‘Download Spreadsheet’
- [28] Masoliver J and Perelló J 2002 *Int. J. Theor. Appl. Finance* **5** 541  
Masoliver J and Perelló J 2002 *Preprint* <http://lanl.arXiv.org/abs/cond-mat/0202203>
- [29] Bouchaud J-P, Matacz A and Potters M 2001 *Phys. Rev. Lett.* **87** 228701
- [30] Muzy J F, Delour J and Bacry E 2000 *Eur. Phys. J. B* **17** 537
- [31] Potters M, Cont R and Bouchaud J-P 1998 *Europhys. Lett.* **41** 239
- [32] Miranda L C and Riera R 2001 *Physica A* **297** 509
- [33] Serva M, Fulco U L, Lyra M L and Viswanathan G M 2002 *Preprint* <http://lanl.arXiv.org/abs/cond-mat/0209103>
- [34] Cizeau P, Liu Y, Meyer M, Peng C-K and Stanley H E 1997 *Physica A* **245** 441  
Liu Y, Gopikrishnan P, Cizeau P, Meyer M, Peng C-K and Stanley H E 1999 *Phys. Rev. E* **60** 1390
- [35] Raberto M, Scalas E, Cuniberti G and Riani M 1999 *Physica A* **269** 148  
Pasquini M and Serva M 2000 *Eur. Phys. J. B* **16** 195
- [36] Miccichè S, Bonanno G, Lillo F and Mantegna R N 2002 *Preprint* <http://lanl.arXiv.org/abs/cond-mat/0202527>
- [37] Friedrich R, Peinke J and Renner C 2000 *Phys. Rev. Lett.* **84** 5224  
Renner C, Peinke J and Friedrich R 2001 *Physica A* **298** 499
- [38] Feynman R P and Hibbs A R 1965 *Quantum Mechanics and Path Integrals* (New York: McGraw-Hill)
- [39] Silva A C and Yakovenko V M 2002 *Preprint* <http://lanl.arXiv.org/abs/cond-mat/0211050>